

## Patchy Particle Model for Vitrimers

Frank Smallenburg,<sup>1,\*</sup> Ludwik Leibler,<sup>2</sup> and Francesco Sciortino<sup>1</sup>

<sup>1</sup>*Department of Physics, Sapienza, Università di Roma, Piazzale Aldo Moro 2, I-00185 Roma, Italy*

<sup>2</sup>*Matière Molle et Chimie, UMR 7167 CNRS-ESPCI, Ecole Supérieure de Physique et Chimie Industrielles,  
10 rue Vauquelin, 75005 Paris, France*

(Received 9 July 2013; published 30 October 2013)

Vitrimers—a recently invented new class of polymers—consist of covalent networks that can rearrange their topology via a bond shuffling mechanism, preserving the total number of network links. We introduce a patchy particle model whose dynamics directly mimic the bond exchange mechanism and reproduce the observed glass-forming ability. We calculate the free energy of this model in the limit of strong (chemical) bonds between the particles, both via the Wertheim thermodynamic perturbation theory and using computer simulations. The system exhibits an entropy-driven phase separation between a network phase and a dilute cluster gas, bringing new insight into the swelling behavior of vitrimers in solvents.

DOI: [10.1103/PhysRevLett.111.188002](https://doi.org/10.1103/PhysRevLett.111.188002)

PACS numbers: 81.05.Lg, 47.57.J-, 82.70.Dd

Vitrimers [1] are a recently invented new class of polymer materials with highly desirable properties, combining malleability and reperability at high temperatures with insolubility. They behave very differently from thermoplastics and thermosets, the two hitherto identified classes of polymers. Thermoplastics made of polymer chains can be reshaped at will, but are soluble, whereas thermosets (or elastomers) made of permanently cross-linked polymers are insoluble and cannot be reshaped once synthesized (cross linked). A vitrimer consists of a covalent organic network that can rearrange its topology via reversible exchange reactions that preserve the total number of network bonds and the average functionality of the nodes. Thanks to network topology rearrangements, stresses in a deformed vitrimer can relax, causing the deformation to become permanent. By the same mechanism, a vitrimer can flow when mechanical stress is applied. On cooling, the exchange reactions slow down and the network topology appears to be fixed on experimental time scales. Thus, a vitrimer behaves like an elastic thermoset (elastomer). On heating, exchange reactions become faster and the viscosity decreases, causing the vitrimer to become malleable. The temperature of this reversible glass transition can be tuned with the aid of a catalyst that controls the exchange reaction rate and activation energy [1–3]. Interestingly, the slowing down of the dynamics near the glass transition closely mimics that of other networked, strong glass-forming liquids, such as germanium dioxide and silica [1–3]. Vitrimers that are based on epoxy resins cured with acids or anhydrides have been shown to be malleable, repairable, recyclable, and insoluble, in addition to being easy to produce from common industrially available ingredients [1,3]. These properties make vitrimers an excellent candidate for applications in, e.g., the aviation, automobile, electronic, and sporting goods industries. Moreover, different exchange reactions and

monomers can be employed to synthesize vitrimers [4–6]. Recently, a continuum model was developed to describe the macroscopic viscoelastic properties of vitrimer networks in terms of the bond exchange reactions [7].

Vitrimers typically consist of two types of monomers with different functionality that can form covalent bonds via a limited number of interaction sites, and as such can be seen as an example of patchy particles. Patchy particle models have been widely used as model systems for particles interacting with specific directional interactions, including water [8,9] and proteins [10–13], and have been studied extensively in recent years, using theory [14,15] and simulations [16–19] as well as experiments [20–26].

In this work, we propose a simple patchy particle model system to study the phase behavior and dynamics of vitrimers. We study it, in the limit of strong (chemical) bonds between the particles, using event-driven molecular dynamics (EDMD) simulations [27], free energy calculations, and the thermodynamic perturbation theory introduced by Wertheim [28,29]. The dynamics of the model directly mimic the bond exchange mechanism present in vitrimers, and reproduce their strong glass-forming ability. We show that the behavior of the material can be quantitatively understood based on a purely entropic model. Our calculations, supported by the simulation results, predict the existence, at low densities, of a region of thermodynamic instability in which the vitrimers phase separate. This phase separation, into a more connected viscoelastic phase coexisting with a gas of small clusters, is the analog of the gas-liquid phase separation in limited valence colloids. The model thus brings a new insight into the behavior of polymer vitrimers in the presence of a solvent and allows us to make interesting predictions concerning the network structure and topology change during swelling.

To design a model system for vitrimers, several requirements have to be satisfied. First, it should be a binary system, which allows for bond formation between the two different species only, with a limited valence for each particle. Second, the bonds between the particles should be highly flexible, and bond switching should be possible without breaking bonds, in order to mimic exchange reactions. In the model proposed here, the monomers in the vitrimer network are represented by the widely used Kern-Frenkel model for patchy particles [30]: interactions between the particles are the combination of a spherical hard-core repulsion with diameter  $\sigma$  and an attraction between the  $f$  attractive patches on the particles. In our case, the system is a mixture of two species of patchy particles, labeled  $A$  and  $B$ , with  $f_A = 4$  and  $f_B = 2$  attractive patches, arranged in tetrahedral and polar geometry, respectively. Two patches can bond (with bonding energy  $\epsilon$ ) if (i) the center-to-center distance between the particles is smaller than the maximum interaction range  $\sigma + \delta = 1.2\sigma$ , and (ii) the vector connecting the centers of the two particles passes through one of the patches on the surface of each of the two particles. The size of the circular patches (and therefore the flexibility of the bonds) is defined by an opening angle  $\theta_m$ , with  $\cos\theta_m = 0.8$ . Note that  $A$  particles can only bond with  $B$  particles, and vice versa. Finally, we impose the restriction that each patch can only be involved in one bond. Whenever a patch has two potential bonding partners available for bonding, our simulations allow for bond switching to mimic bond exchange reactions in the vitrimer system (see Fig. 1) [27]. We denote the number of particles of species  $i$  with  $N_i$ , the volume with  $V$ , and the composition with  $x = N_A/(N_A + N_B)$ . Time is measured in units of  $\tau \equiv \sqrt{\beta m \sigma^2}$ , with  $m$  the mass of a particle, and  $\beta = 1/k_B T$ , with  $k_B$  Boltzmann's constant and  $T$  the temperature. In the vitrimer system, after mixing the two components, all possible covalent bonds allowed by

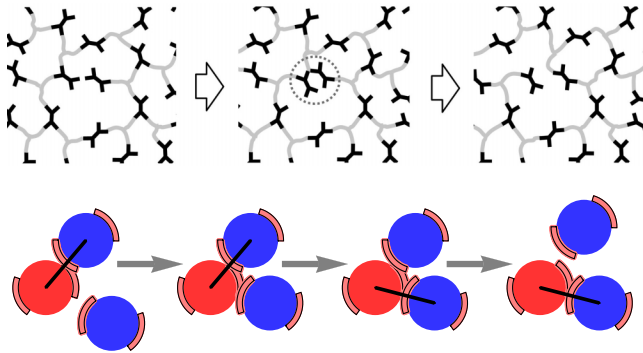


FIG. 1 (color online). Cartoon of the bond-switching mechanism in vitrimers (top, reproduced from Ref. [1]) and the corresponding patchy particle model (bottom). In both cases, network reorganization can take place by a bonding site switching from its current bonding partner to another nearby free interaction site of the right species. Note that bonds are only possible between particles of different types (denoted by color).

the stoichiometry of the mixture form. The subsequent switching of covalent bonds between monomers occurs via bond exchange reactions. Thus, it is this bond switching that controls the dynamics of the system. In order to mimic the covalent nature of the  $A$ - $B$  bonds, we perform our EDMD simulations at  $T \approx 0$ , where bonds never break. Starting from a randomly chosen configuration, the system quickly evolves toward a fully bonded state, where all possible bonds are formed [i.e., when the total number of bonds  $n_b$  in the system is equal to  $\min(f_A N_A, f_B N_B)$ ]. Subsequently, network rearrangement only occurs via bond switching. Thus, after equilibration, the number of bonds in the system is maximized at all times. The bond switching rate can be externally adjusted to model the dynamics of the network at different temperatures, or (equivalently) different degrees of catalyst effectiveness. The wide bonding angle in the model and the corresponding large entropy associated with the formation of a bond is instrumental in reaching the fully bonded state, preventing entropic bottlenecks.

Following Wertheim [28,29], to calculate the Helmholtz free energy  $F_{\text{tot}}$  of the system, we break it down into three parts: the free energies associated with the hard-sphere reference system ( $f_{\text{HS}}$ ), forming the bonds ( $f_{\text{bond}}$ ), and mixing the two species ( $f_{\text{mix}}$ ). Thus,

$$\beta F_{\text{tot}}/N = \beta f_{\text{bond}} + \beta f_{\text{HS}} + \beta f_{\text{mix}}, \quad (1)$$

where

$$\beta f_{\text{bond}} = x[4 \log(1 - p_A) + 2p_A] + (1 - x) \times [2 \log(1 - p_B) + p_B], \quad (2)$$

$$\beta f_{\text{HS}} = \log(\rho \Lambda^3) - 1 + \frac{4\phi - 3\phi^2}{(1 - \phi)^2}, \quad (3)$$

$$\beta f_{\text{mix}} = x \log(x) + (1 - x) \log(1 - x), \quad (4)$$

with  $\eta$  the hard-sphere packing fraction and  $p_A$  ( $p_B$ ) the probability that a patch on a particle of type  $A$  ( $B$ ) is bonded.

The bonding free energy ( $f_{\text{bond}}$ ) can be calculated from the total number  $n_b$  of bonds in the system, which can be calculated using the law of mass action describing a chemical equilibrium between bonded and unbonded sites:

$$\frac{n_b}{(f_A N_A - n_b)(f_B N_B - n_b)} = \frac{\Lambda^3}{V} e^{-\beta \mathcal{F}_b}, \quad (5)$$

where  $\mathcal{F}_b$  is the free energy of the formation of a bond, and  $\Lambda^3$  is the thermal wavelength of a particle.

Wertheim theory [28,29] provides an expression for  $\mathcal{F}_b$ , calculated by integrating over the bonding volume for two specific wells on two particles. For the Kern-Frenkel model, this can be written as

$$e^{-\beta\mathcal{F}_b} = \frac{v_b(\rho)}{\Lambda^3} [\exp(-\beta\epsilon) - 1], \quad (6)$$

where the bonding volume  $v_b(\rho)$  is determined via an integral of the hard-sphere radial distribution function over the bonding volume [see Supplementary Material (SM) [31]]. The number of bonds directly provides the potential energy, which is given by  $U = -n_b\epsilon$ . In the limit of chemical bonds ( $\epsilon \gg k_B T$ ), the number of bonds  $n_b$  is always maximized:

$$n_b = \min(f_A N_A, f_B N_B). \quad (7)$$

This fully bonded case, appropriate for the description of (covalently bonded) vitrimers, is particularly interesting, since the entire transition is driven by entropy, analogous to hard spheres. In this specific case, the bonding free energy is given by (see SM [31] for details)

$$f_{\text{bond}} = -\frac{TS_{\text{comb}}(4N_A, 2N_B)}{N} - \frac{n_b}{N} \left( \mathcal{F}_b \log \frac{\Lambda^3}{V} \right), \quad (8)$$

where

$$S_{\text{comb}}(n, m) = \begin{cases} k_B \log(n!/(n-m)!) & \text{if } n > m \\ k_B \log(m!/(m-n)!) & \text{otherwise} \end{cases} \quad (9)$$

corresponds to the entropy associated with the number of ways a number of (distinguishable) bonds can be distributed over a larger number of patches, and is therefore associated with the configurational entropy in the system. The last term in Eq. (8) represents the change in vibrational free energy from creating a bond, multiplied by the number of bonds  $n_b$ . Therefore,  $F_{\text{tot}}$  can be written as the (fixed) total energy  $U$  associated with the bonds ( $U = -n_b\epsilon$ ) plus a remaining purely entropic  $-TS_{\text{tot}}$  term:

$$\frac{S_{\text{tot}}}{N} = s_{\text{HS}} + s_{\text{mix}} + \frac{S_{\text{comb}}}{N} + \frac{k_B n_b}{N} \log \frac{v_b(\rho)}{V}, \quad (10)$$

where  $s_{\text{HS}} = -k_B \beta f_{\text{HS}}$  and  $s_{\text{mix}} = -k_B \beta f_{\text{mix}}$ . In fact, because the system always maximizes  $n_b$ , the deciding factor in the phase behavior is entropy, rather than energy, despite the low temperature. While the Wertheim expression for  $S_{\text{tot}}$  in Eq. (10) is very simple, Fig. 2 shows that it agrees very well with the “exact” entropy calculated from simulations.

Knowing the free energy of the system at arbitrary  $x$ ,  $\rho$ , and  $T$ , we can calculate phase coexistences in the binary mixture. To do this, we calculate the Gibbs free energy  $G = F + PV$  per particle at constant pressure  $P \equiv -\partial F / \partial V|_{N_A, N_B, T}$  and temperature  $T$ , as a function of the composition, and obtain coexisting points by using a standard common-tangent construction [32].

In addition to the theoretical calculations, we use computer simulations and thermodynamic integration to determine the free energy of the fluid phase in the patchy particle model system in the zero- $T$  limit, where the number of bonds is fixed to its maximum value. To calculate the

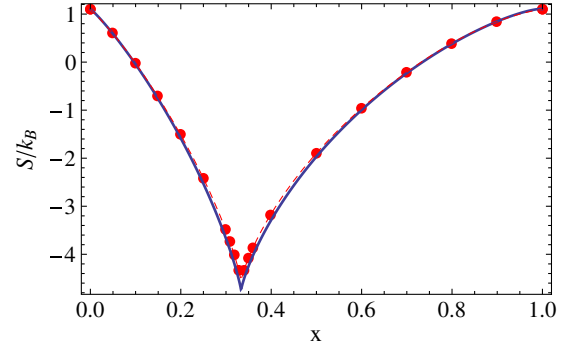


FIG. 2 (color online). Entropy  $S = (F_{\text{tot}} - U)/T$  per particle at  $T = 0$  and  $\rho\sigma^3 = 0.35$ . The red points indicate simulation results (thermodynamic integration) and the blue line theoretical predictions (Wertheim). The fitted red dashed line is used to calculate free energies for drawing the phase diagram.

free energy at each state point, we measure the derivatives of the free energy ( $U$  and  $P$ ) directly in EDMD simulations [27] in the canonical ( $NVT$ ) ensemble and integrate the results [33]. As reference free energies we use the hard-sphere Carnahan-Starling equation of state for the denser fluids and the Wertheim theory described in the previous section in the dilute gas limit ( $\rho\sigma^3 < 10^{-3}$ ), where the approximations made are accurate. While no crystal phases were explored, we do not expect any crystal phase to be relevant at these densities: earlier work [27] has shown that combining large bond flexibility (as is present here) with limited valence strongly suppresses the stability of low-density crystal structures.

The phase diagrams obtained from the simulations (points) and theory (dashed line) are shown in Fig. 3, as a function of  $\rho$  and  $x$ . We observe remarkable agreement with the theoretical predictions. The main difference is a slight underestimation of the theory for the coexistence density of the high-density fluid, as is common for Wertheim theory [14]. The phase diagram shows a large coexistence region, where the system—retaining the same number of bonds—phase separates into two phases, as indicated by the tie lines.

Since solvents are not explicitly taken into account in our model, the phase diagram represents the behavior of vitrimers in a good solvent: lowering the density in the model system is equivalent to the addition of solvent to the vitrimer system, and favors the formation of a dilute phase consisting of small clusters. The calculated phase diagram demonstrates that vitrimers can never be fully dissolved. While dilution will allow some material to escape from the network to a gaslike phase, the tie lines in Fig. 3 show that the remaining network is always closer to the optimal composition  $x_{\text{id}}$ , while the escaped material consists mainly of the “excess” species. Thus, diluting the network phase (i.e., putting it into contact with a good solvent) will always push the system towards a more fully bonded network, while monomers and small clusters escape into

the solvent. However, as also seen in experiments [1], the network phase never fully dissolves: as the network approaches  $x_{id}$ , less and less material will be able to escape the network.

We reemphasize here that the phase separation is driven purely by entropy, under the constraint of a maximized number of bonds. The phase separation arises essentially from the possibility of forming bonds inside the percolating network, generating one additional free cluster in the dilute phase that gains a significant fraction of translational entropy. Indeed, consider the case where  $x < x_{id}$ , so that all clusters are “terminated” by  $B$  particles. Joining two clusters via bond exchange expels a  $B$  particle, leaving the total number of clusters constant, with no translational entropic gain. However, forming an intracluster bond (a ring) also expels a  $B$  particle, but this time increases the total number of clusters by one, increasing the translational entropy in the system. This is balanced by an decrease of configurational entropy in the network [i.e.,  $S_{mix}$  and  $S_{comb}$  in Eq. (10)]. However, at low density, where the translational entropy of a free cluster is large, maximization of entropy favors the phase separation seen in Fig. 3. For the same reason, our simulations show the spontaneous merging of fully bonded clusters at high bond switching rates, demonstrating not only that separate pieces of material can be joined together but also that even in the ground state, coalescence is thermodynamically favorable (see movie in SM [31]). After two clusters link, the number of bonds between the two clusters gradually increases via bond exchange reactions, until a single, homogeneous cluster remains. This directly parallels the observed ability of vitrimers to resolve breaks and other damage when the bond switching rate is high, as well as the

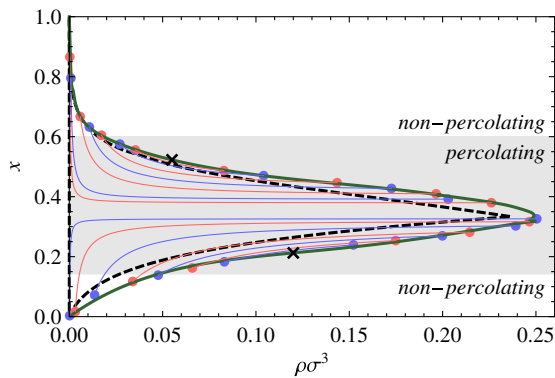


FIG. 3 (color online). Comparison between the phase diagram obtained from simulations (points and tie lines) and the one obtained from Wertheim theory (dashed line) at  $T = 0$ . The solid line is a fit to the coexistence points, indicating the instability region. The blue and red lines (colored to improve visibility) indicate tie lines, i.e., the set of  $\rho - x$  values that phase separate in the same two coexisting states. The shaded region denotes the region where percolation is expected (i.e., where theory predicts that  $p_{APB} = 1/3$  [38]). The black crosses indicate the approximate critical points for the simulation data.

possibility to recycle the material by breaking up the material into small pieces and melting them together at a high temperature [1].

We now turn to the dynamics in the system. The key ingredient for the material properties of the vitrimer system is the bond switching mechanic [7], which allows the network to rearrange its topology despite the covalent nature of the bonds. The rate of bond switching ( $\gamma$ ) is controlled by  $T$ . Effectively,  $\gamma$  is proportional to  $\exp(-\epsilon_a/k_B T)$  for an activation energy  $\epsilon_a$ .  $\epsilon_a$  and the prefactor can be tuned by modifying the catalyst and its concentration [2,7]. Since the bond switching mechanic is the limiting factor for the dynamics at low  $T$  [27], the shear viscosity  $\eta$  increases exponentially (Arrhenius-like) with decreasing  $T$  ( $\eta \propto \gamma^{-1}$ ) so that vitrimers can be classified as strong glass formers [34,35]. In the simulations of the patchy particle model, the bond switching rate  $\gamma$  is explicitly imposed. For a given  $\gamma$ , each patch will attempt on average  $\gamma t$  switches over a time  $t$  [27]. It should be noted that the phase diagram is independent of  $\gamma$ . To compare the dynamics in our model system to experimental results, we calculate  $\eta$  by measuring correlations in the off-diagonal components of the stress tensor (see SM [31]) [36,37]. Figure 4 shows  $\eta$  as a function of  $\gamma^{-1}$ . While the dynamics become independent of  $\gamma$  when the time between bond switching events is short compared to the motion of the particles [ $(\gamma\tau)^{-1} \ll 1$ ], the viscosity shows a clear linear behavior for long bond switching times  $(\gamma\tau)^{-1} \gtrsim 1$ . As proposed for vitrimers [3], the observed behavior for large  $(\gamma\tau)^{-1}$  confirms that the dynamics become slaved to the switching microscopic time scale, offering a possible interpretation for the origin of the strong behavior of molecular glass formers.

In short, the system proposed in this paper provides a simple model for vitrimers, providing direct insight into the physics involved in their qualitative behavior. The model faithfully captures the bond exchange mechanism, which allows the system to rearrange its network topology

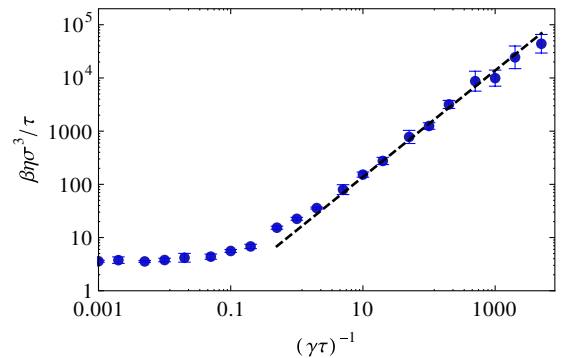


FIG. 4 (color online). Dimensionless shear viscosity  $\beta\eta\sigma^3/\tau$  as a function of the average time interval between bond switching events  $(\gamma\tau)^{-1}$ . The dashed line indicates an Arrhenius law (slope 1). The viscosities were calculated at  $x = 0.25$  and  $\rho\sigma^3 = 0.35$ , well away from the area where phase separation occurs.

at high bond-switching rates (corresponding to high  $T$  and catalyst concentrations), without ever leaving the energetic ground state, where the maximum number of bonds are formed. By reproducing the bond switching mechanism, the model system not only mimics the possibility to repair or recycle vitrimers at high temperatures but also directly captures the strong glass-forming ability shown in vitrimers. The phase behavior is well described by Wertheim theory, providing predictions for the phase coexistences and cluster size distributions in the experimental vitrimer system. Interestingly, the model predicts that in contact with a solvent reservoir, the vitrimer network does not dissolve but instead expels particles and changes its composition, approaching a defect-free state.

We acknowledge support from ERC-226207-PATCHYCOLLOIDS and MIUR-PRIN.

\*Corresponding author.

f.smallenburg@gmail.com

- [1] D. Montarnal, M. Capelot, F. Tournilhac, and L. Leibler, *Science* **334**, 965 (2011).
- [2] M. Capelot, D. Montarnal, F. Tournilhac, and L. Leibler, *J. Am. Chem. Soc.* **134**, 7664 (2012).
- [3] M. Capelot, M. M. Unterlass, F. Tournilhac, and L. Leibler, *ACS Macro Lett.* **1**, 789 (2012).
- [4] Y.-X. Lu, F. Tournilhac, L. Leibler, and Z. Guan, *J. Am. Chem. Soc.* **134**, 8424 (2012).
- [5] P. Zheng and T. J. McCarthy, *J. Am. Chem. Soc.* **134**, 2024 (2012).
- [6] C. J. Kloxin and C. N. Bowman, *Chem. Soc. Rev.* **42**, 7161 (2013).
- [7] R. Long, H. J. Qi, and M. L. Dunn, *Soft Matter* **9**, 4083 (2013).
- [8] J. Kolafa and I. Nezbeda, *Mol. Phys.* **61**, 161 (1987).
- [9] F. Romano, P. Tartaglia, and F. Sciortino, *J. Phys. Condens. Matter* **19**, 322101 (2007).
- [10] H. Liu, S. K. Kumar, and F. Sciortino, *J. Chem. Phys.* **127**, 084902 (2007).
- [11] C. Gögelein, G. Nägele, R. Tuinier, T. Gibaud, A. Stradner, and P. Schurtenberger, *J. Chem. Phys.* **129**, 085102 (2008).
- [12] J. P. Doye, A. A. Louis, I.-C. Lin, L. R. Allen, E. G. Noya, A. W. Wilber, H. C. Kok, and R. Lyus, *Phys. Chem. Chem. Phys.* **9**, 2197 (2007).
- [13] N. Dorsaz, L. Filion, F. Smallenburg, and D. Frenkel, *Faraday Discuss.* **159**, 9 (2012).
- [14] E. Bianchi, J. Largo, P. Tartaglia, E. Zaccarelli, and F. Sciortino, *Phys. Rev. Lett.* **97**, 168301 (2006).
- [15] E. Bianchi, R. Blaak, and C. N. Likos, *Phys. Chem. Chem. Phys.* **13**, 6397 (2011).
- [16] D. de las Heras, J. M. Tavares, and M. M. Telo da Gama, *Soft Matter* **8**, 1785 (2012).
- [17] F. Sciortino, *Eur. Phys. J. B* **64**, 505 (2008).
- [18] F. J. Martinez-Veracoechea, B. M. Mladek, A. V. Tkachenko, and D. Frenkel, *Phys. Rev. Lett.* **107**, 045902 (2011).
- [19] F. Romano and F. Sciortino, *Nat. Commun.* **3**, 975 (2012).
- [20] Y. Wang, Y. Wang, D. R. Breed, V. N. Manoharan, L. Feng, A. D. Hollingsworth, M. Weck, and D. J. Pine, *Nature (London)* **491**, 51 (2012).
- [21] B. Ruzicka, E. Zaccarelli, L. Zulian, R. Angelini, M. Sztucki, A. Moussad, T. Narayanan, and F. Sciortino, *Nat. Mater.* **10**, 56 (2011).
- [22] S. Biffi, R. Cerbino, F. Bomboi, E. Maria Paraboschi, R. Asselta, F. Sciortino, and T. Bellini *Proc. Natl. Acad. Sci. U.S.A.* **110**, 15633 (2013).
- [23] X. Mao, Q. Chen, and S. Granick, *Nat. Mater.* **12**, 217 (2013).
- [24] Q. Chen, S. C. Bae, and S. Granick, *Nature (London)* **469**, 381 (2011).
- [25] S. Jiang, Q. Chen, M. Tripathy, E. Luijten, K. S. Schweizer, and S. Granick, *Adv. Mater.* **22**, 1060 (2010).
- [26] A. B. Pawar and I. Kretzschmar, *Macromol. Rapid Commun.* **31**, 150 (2010).
- [27] F. Smallenburg and F. Sciortino, *Nat. Phys.* **9**, 554 (2013).
- [28] M. S. Wertheim, *J. Stat. Phys.* **35**, 19 (1984).
- [29] M. S. Wertheim, *J. Stat. Phys.* **35**, 35 (1984).
- [30] N. Kern and D. Frenkel, *J. Chem. Phys.* **118**, 9882 (2003).
- [31] See Supplemental Material at <http://link.aps.org/supplemental/10.1103/PhysRevLett.111.188002> for additional details on the derivation of the free energy, phase diagrams for different parameter choices, details on the viscosity measurements, an explanation of the entropy change associated with cluster coalescence, and a movie of a simulation of two merging clusters.
- [32] D. de las Heras, J. M. Tavares, and M. M. Telo da Gama, *Soft Matter* **7**, 5615 (2011).
- [33] D. Frenkel and B. Smit, *Understanding Molecular Simulations: From Algorithms to Applications* (Academic Press, San Diego, CA, 2002).
- [34] C. A. Angell, *Science* **267**, 1924 (1995).
- [35] P. G. Debenedetti, *Metastable Liquids: Concepts and Principles* (Princeton University Press, Princeton, NJ, 1996).
- [36] B. J. Alder, D. M. Gass, and T. E. Wainwright, *J. Chem. Phys.* **53**, 3813 (1970).
- [37] A. M. Puestas, C. De Michele, F. Sciortino, P. Tartaglia, and E. Zaccarelli, *J. Chem. Phys.* **127**, 144906 (2007).
- [38] P. J. Flory, *J. Am. Chem. Soc.* **63**, 3083 (1941).